Toxicology in Vitro 32 (2016) 297–309

Contents lists available at ScienceDirect

Toxicology in Vitro

journal homepage: www.elsevier.com/locate/toxinvit

Benzyl butyl phthalate promotes adipogenesis in 3T3-L1 preadipocytes: A High Content Cellomics and metabolomic analysis

Lei Yin, Kevin Shengyang Yu [1], Kun Lu, Xiaozhong Yu *

Department of Environmental Health Science, University of Georgia, Athens, GA, United States

ARTICLE INFO

Article history:
Received 8 September 2015
Received in revised form 12 January 2016
Accepted 20 January 2016
Available online 25 January 2016

Keywords:
Benzyl butyl phthalate
Adipogenesis
High Content Cellomics analysis (HCA)
Gene expression
Metabolomic analysis

ABSTRACT

Benzyl butyl phthalate (BBP) has been known to induce developmental and reproductive toxicity. However, its association with dysregulation of adipogenesis has been poorly investigated. The present study aimed to examine the effect of BBP on the adipogenesis, and to elucidate the underlying mechanisms using the 3T3-L1 cells. The capacity of BBP to promote adipogenesis was evaluated by multiple staining approaches combined with a High Content Cellomics analysis. The dynamic changes of adipogenic regulatory genes and proteins were examined, and the metabolite profile was identified using GC/MC based metabolomic analysis. The High Content analysis showed BBP in contrast with Bisphenol A (BPA), a known environmental obesogen, increased lipid droplet accumulation in a similar dose-dependent manner. However, the size of the lipid droplets in BBP-treated cells was significantly larger than those in cells treated with BPA. BBP significantly induced mRNA expression of transcriptional factors C/EBPα and PPARγ, their downstream genes, and numerous adipogenic proteins in a dose and time-dependent manner. Furthermore, GC/MC metabolomic analysis revealed that BBP exposure perturbed the metabolic profiles that are associated with glyceroneogenesis and fatty acid synthesis. Altogether, our current study clearly demonstrates that BBP promoted the differentiation of 3T3-L1 through the activation of the adipogenic pathway and metabolic disturbance.

1. Introduction

Obesity is a growing health problem and has been found to be closely associated with increased risk of various disease development (Allender and Rayner, 2007; Hossain et al., 2007; Hursting and Dunlap, 2012; McTigue et al., 2014; Stanner and Yudkin, 2001; Swinburn et al., 2011). Accumulating evidence suggests that exposure to environmental chemicals, also termed "obesogens", may alter human metabolism, predispose some people to gain weight, and contribute to the development of obesity and metabolic disorders (Baillie-Hamilton, 2002; Janesick and Blumberg, 2011; Newbold et al., 2009).

Phthalates are commonly used as plasticizer in polyvinyl chloride (PVC) plastics, and therefore, are found in numerous household products such as food packaging, furniture, toys and even in medical devices such as tubing and intravenous bags. Phthalates can enter the body through inhalation, ingestion, dermal exposure, and can be rapidly degraded into the respective phthalate monoesters, and eliminated in the urine. Metabolites of phthalates have been detected in human serum and urine, and the levels of these metabolites have been found to be associated with increased insulin resistance, decreased insulin sensitivity, and impaired beta cell function in overweight and obese populations (Frederiksen et al., 2007; Gray et al., 2000; Heudorf et al., 2007; Koch et al., 2006; Wittassek and Angerer, 2008; Yaghjyan et al., 2015). Although phthalates have been identified to have anti-androgenic effects on the developing male reproductive system (Foster, 2006; Shultz et al., 2001; Wolff et al., 2014), emerging evidence suggests a potential connection with the development of obesity (Desvergne et al., 2009; Grun and Blumberg, 2007; Hatch et al., 2008; Kim and Park, 2014; Newbold et al., 2009; Song et al., 2014; Stahlhut et al., 2007; Teitelbaum et al., 2012). Epidemiology studies have revealed a potential association between phthalate exposures such as diethylhexyl phthalate (DEHP) and the development of obesity (Buser et al., 2014; Hatch et al., 2008; Lind et al., 2012; Stahlhut et al., 2007; Teitelbaum et al., 2012; Trasande et al., 2013). In the National Health and Nutrition Examination Survey (NHANES) from 1999 to 2002, concentrations of four phthalate metabolites, including mono-benzyl phthalate (MBzP), mono-(2-ethyl-5-hydroxyhexyl) phthalate (MEHHP), mono-(2-ethyl-5-oxohexyl) phthalate (MEOHP), and mono-ethyl phthalate (MEP) in men, showed significant correlations with abdominal obesity (Stahlhut et al., 2007). In addition, three phthalate metabolites, including mono-butyl phthalates (MBP), MBzP, and MEP showed significant correlations with the increased insulin

* Corresponding author at: Department of Environmental Health Science, College of Public Health, University of Georgia, EHS Bldg., 150 Green Street, Athens, GA 30602, United States.
E-mail address: yuxz@uga.edu (X. Yu).
[1] Current address: Bioengineering, California Institute of Technology, Pasadena CA 91125.

http://dx.doi.org/10.1016/j.tiv.2016.01.010
0887-2333/

resistance. Recently, significant increases of phthalic acid (PA) and phthalates [mono-ethyl (MEP), di-*n*-butyl (DBP) in both urine and serum were found in young obese girls, suggesting the potential correlation between phthalate esters exposure and the development of obesity (Choi et al., 2014). Moreover, perinatal exposure to monoethylhexyl-phthalate (MEHP), a major metabolite of DEHP in mice, was found to perturb key regulators of adipogenesis and lipogenic pathways (Hao et al., 2012), to promote PPARγ activity and to increase the incidence of obesity during fetal development (Hurst and Waxman, 2003; Latini et al., 2006).

Benzyl butyl phthalate (BBP) has been characterized as an endocrine disruptor, a hormonally active compound linked to reproductive toxicity and neurotoxicity, in both animals and humans (Agas et al., 2007; Gray et al., 2000; Harris et al., 1997; Nativelle et al., 1999; Picard et al., 2001; Piersma et al., 2000; Swan, 2008; Weiss, 2012). BBP exposure has been found to be associated with increased risks of various diseases, such as asthma in children (Shin et al., 2014; Whyatt et al., 2014), endometriosis (Reddy et al., 2006), and malformations of sexual differentiation (Agas et al., 2007; Gray et al., 2000). BBP treatment has also been reported to activate PPARγ (Pereira-Fernandes et al., 2013; Pereira-Fernandes et al., 2014). So far, neither epidemiological study, nor *in vivo* animal experiment has revealed that BBP exposure is associated with the development of obesity. The purpose of this study is to investigate whether BBP exposure could affect adipogenesis using an *in vitro* 3T3-L1 murine preadipocyte model as well as its underlying molecular mechanism. We measured the lipid droplet accumulation qualitatively or quantitatively using Oil Red O or Nile red staining, respectively. We further applied a neutral lipid stain, LipidTox, to characterize the potential effects of BBP on lipid metabolism using a cell-based High Content Cellomics assay. We examined the underlying molecular mechanism of pathways involved in adipogenesis by measuring the dynamic expression of these regulatory genes. Finally, we applied a GC/MC metabolomic tool to explore the potential metabolic molecules involved in adipogenesis. Our current study has demonstrated that BBP exposure significantly promoted lipid droplet accumulation and intracellular triglyceride production in a dose-dependent manner. BBP induced adipogenesis through the alterations of dynamic changes of transcriptional factors, such as C/EBPα and PPARγ, adipogenic-specific genes such as AdipoQ, Adipsin, FABP4, LPL and FASN as well as the perturbation of metabolites that are associated with glyceroneogenesis and fatty acid synthesis. Our established Cellomics-based high-throughput screening approach will be invaluable for a first line screening for environmental obesogens (OECD, 2012).

2. Materials and methods

2.1. Chemicals and reagents

Dulbecco's modified Eagle's medium (DMEM), antibiotics (penicillin and streptomycin), fetal bovine serum (FBS), and 0.25% trypsin were purchased from GE Healthcare Life Sciences (Logan, Utah). Insulin, dexamethasone (DEX), 3-isobutyl-1-methylxanthine (IBMX), benzyl butyl phthalate (BBP), Bisphenol A (BPA), protease inhibitor cocktail, Dimethyl sulfoxide (DMSO), and neutral red were purchased from Sigma (St. Louis, MO).

2.2. 3T3-L1 cell culture

3T3-L1 mouse preadipocyte was kindly gifted from Dr. Cliffton Baile's laboratory at the University of Georgia. Cells were maintained in DMEM composed of high glucose, 10% FBS, and 100 U/ml penicillin and streptomycin in a 37 °C, 5% CO_2 humidified environment as previously described (Brady et al., 1999). The cultured cells were maintained at a sub-confluence condition with media changes every 2–3 days.

2.3. 3T3-L1 differentiation and treatments

The protocol for the differentiation of adipocytes was followed as previously reported (Madsen et al., 2003; Zebisch et al., 2012). As shown in Fig. 1, 3T3-L1 cells were cultured to 100% confluence in 10% FBS DMEM (M1 medium), denoted as day 0 either in 96 well-plate, or 12 well-plate, or 35 mm dish for various endpoints of examinations. After post-confluence, cells were incubated in adipogenic induction medium (M2 medium: DMEM containing 1 μM DEX, 0.5 mM IBMX, 167 nM insulin and 10% FBS) for 2 days (day 2). Cells were then cultured in adipogenic differentiation medium (M3 medium: DMEM containing 167 nM insulin and 10% FBS) for another 2 days (day 4), followed by DMEM with 10% FBS (M1) for another 4 days (day 8). The cells cultured with M2 medium for 2 days, M3 medium for 2 days and M1 medium for 4 days were used as positive controls. We applied this standardized protocol to ensure the ability of cells to differentiate. In this study, BPA, a known environmental obesogen, was included as a comparison to evaluate the adipogenic effects. To examine the effects of these compounds on the adipogenesis of 3T3-L1, BBP or BPA was added to M2 medium without DEX for 2 days, M3 medium for 2 days, and M1 medium for another 4 days. Cells with only the vehicle (DMSO 0.1%) in M1, M2, and M3 media were set as the untreated control (NC1), while cells cultured with the medium containing M2 but lacking DEX during the first 2 days were used as another negative control (NC2).

2.4. Neutral red uptake assay

In order to select doses of BBP without affecting the cell viability of the 3T3-L1 preadipocyte, a neutral red uptake assay was used to measure the cell viability after treatments with BBP (Repetto et al., 2008; Yu et al., 2009). Briefly, 3T3-L1 preadipocytes were cultured in a 96-well plate to 80% confluence, and treated with various doses of BBP for 24 and 48 h. The quantity of dye incorporated into cells was measured by spectrometry at 540 nm (Gen5, BioTek), and the cell viability was calculated as the ratio of the treatment *versus* control. The data represented the average ± standard deviation of six replicates, and were expressed as a fold change of the treated *versus* untreated control.

2.5. Oil Red O staining and quantification of triglyceride content

3T3-L1 cells were seeded in 12-well plates, and treated with BBP or BPA at indicated concentrations from day 0 to day 8. On day 8, cells were fixed in fresh 4% paraformaldehyde (pH 7.4) and the intracellular lipid droplets were stained with a filtered solution of 60% Oil Red O in 100% 2-isopropanol, as previously described (Suryawan and Hu, 1993). Quantification of intracellular triglyceride content in the cells was stained with Nile red using AdipoRed™ Assay according to the manufacturer's instructions (Lonza, MD), the fluorescence intensity was measured at 572 nm (Gen5, BioTek) The experiment was performed with four technical replicates and repeated three times.

2.6. Automated quantification of lipid droplets using cellomics high content analysis

3T3-L1 cells were seeded in a black frame 96-well plate (Corning, NY), and treated with BBP or BPA as indicated concentrations from day 0 to day 8. Cells were then fixed with 4% paraformaldehyde, followed by washing with PBS twice. A mixed PBS solution containing Hoechst 33342 (1 μM) for nuclear staining, and LipidTOX for neutral lipid staining (Life Technologies, NY) was added to each well, and the plate was incubated at room temperature for 30 min. Lipid droplets were quantified with the Cellomics® ArrayScan® VTI HCS Reader with HCS Studio™ 2.0 Cell Analysis Software (Thermo Scientific, MA). Lipid droplets were

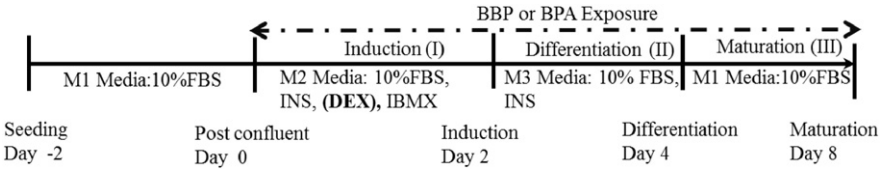

Fig. 1. Overview of the experiment setup of differentiation and treatments in preadipocyte 3T3-L1. 3T3-L1 cells were cultured to 100% confluence in 10% FBS DMEM (M1 medium), denoted as day 0. To differentiate the pre-adipocyte 3 T3-L1 cells as a positive control (Pos), cells were incubated in adipogenic induction medium (M2 medium: DMEM containing 1 μM DEX, 0.5 mM IBMX, 167 nM insulin and 10% FBS) for 2 days (day 2). Cells were then cultured in adipogenesis differentiation medium (M3 medium: DMEM containing 167 nM insulin and 10% FBS) for another 2 days (day 4), followed by M1 for another 4 days for maturation (day 8). To examine the effect of compound on the adipogenesis, BBP or BPA was added to M2 medium for two days without DEX, M3 medium for two days, and M1 medium for another four days. Cells cultured with the vehicle (DMSO 0.1%) in all medium was set as the untreated control (NC1), while cells cultured with the M2 medium without DEX during the first 2 days was indicated as another negative control (NC2).

detected with the provided SpotDetector® BioApplication. A fluorescent dye, LipidTOX, was used to visualize and quantify lipid droplets in the differentiated adipocytes, while the nuclei were stained using Hoechst 33342 dye. The method is based on a two-channel assay, which uses a 20× objective (NA 0.5), a Hamamatsu ORCA-ER digital camera in combination with a 0.63× coupler and Carl Zeiss microscope optics for automatic image acquisition. Images were acquired in high resolution (1024 × 1024) and auto focus mode. Channel one applies the BGRFR 386-23 for Hoechst 33342, which was the focus channel, and the objects (nuclei) were identified. The spots (lipid droplets) were detected in channel two (BGRFR 549-15 filter). The default settings of the SpotDetector algorithm version 4.1 were altered such that, in channel 2 for the LipidTox, thresholds were set to ensure that these droplets and intensity were selected for analysis of 40 fields per well. The data of each channel were reported on a "per field" basis. Lipid spot counts and intensity of spot counts were normalized to the number of nucleus; and total lipid intensity per spot (average spot volume) were calculated. The experiment was performed with 8 technical replicates and repeated three times.

2.7. RNA isolation and quantitative real-time RT-PCR (QRT-PCR)

3T3-L1 cells were treated with BBP with the indicated doses for various periods as shown in Fig. 1. Total RNAs were isolated at day 2 (induction stage), day 4 (differentiation stage), and day 8 (maturation stage). The quality and quantity of total RNA were measured on a Nanodrop (Thermo Scientific, MA). cDNA was reverse-transcribed from 2 μg total RNA using iScript Reverse Transcription (BioRad, Hercules, CA). Quantitative realtime RT-PCR was conducted using an aliquot of the synthesized cDNA with SsoAdvanced Universal SYBR Green Supermix (BioRad, CA). The amplification conditions were initial denaturation at 95 °C for 10 min, followed by 40 cycles of denaturation at 95 °C for 30 s, annealing at 55–57 °C for 30 s and elongation at 72 °C for 30 s. Melt-curve analysis was performed to confirm that the signal was that of the expected amplification product and not of possible primer-dimers. Oligonucleotide primers were designed according to the published sequences or using Primer 3.0 software and UCSC Genome Bioinformatics (http://frodo.wi.mit.edu/cgi-bin/primer3/primer3-www.cgi; http://genome.ucsc.edu/). The sequences of oligonucleotide primers are listed in Table 1. Each sample was normalized to the level of the glyceraldehydes-3-phosphate dehydrogenase (GAPDH) transcript and the relative fold change were conducted as described previously (Yin and Dale, 2007). Results are expressed as the relative fold change of treatment over the control. Three independent experiments were performed, and each test condition was conducted in triplicates.

2.8. Protein extraction and western blot analysis

3T3-L1 cells were treated with indicated concentrations of BBP, BPA, or control media, and then harvested and lysed with ice-cold cell lysis buffer from Cell Signaling Technology (Boston, MA). The cell lysates were sonicated on ice and the soluble materials were collected from the supernatants after centrifugation at 13,000 rpm for 15 min at 4 °C. The protein concentration was determined according to the manufacturer's instructions (BioRad, CA). Equal amounts of total protein (10 μg) were resolved by 4–12% Bis-Tris polyacrylamide gel electrophoresis and transferred to a polyvinylidene difluoride (PVDF) membrane (Millipore, MA). Western blot analyses were performed with monoclonal rabbit antibodies against PPARγ, C/EBPα, Acetyl-CoA Carboxylase (CoA), Adiponectin, FABP4, Fatty Acid Synthase (FASN), Perilipin (Cell Signaling, MA), and housekeeping protein beta-actin (Santa Cruz Biotechnology, Santa Cruz, CA) for overnight at 4 °C. The blots were washed five times with Tris-buffered saline containing 0.05% Tween 20 (TBS-T), and were then incubated with a horseradish peroxidase conjugated secondary anti-mouse antibody (Jackson Immuno Research, PA), or anti-rabbit IgG, HRP-linked Antibody (Cell Signaling, MA) for 1.5 h at room temperature. Immunoreactivity bands were visualized by enhanced chemiluminescence (BioRad, CA). The bands were quantified by densitometric analysis Image J 1.49 (NIH).

2.9. Gas chromatography–mass spectrometry (GC/MC) based metabolomic analysis

3T3-L1 cells were inoculated in 35 mm dishes, and treated with indicated concentrations of BBP from day 0 through day 8. Cells were washed twice with PBS prior to being quenched with 80% cold methanol, and subsequently suspended in methanol. Following the quench, the methanol supernatant was evaporated from the cells, and the remaining cellular pellets were extracted using a mixture of methanol, deionized water and chloroform (CCl3). Briefly, 485 μl of a 58% MeOH solution and 400 μl CCl3 were added stepwise. After lysis and centrifugation, the supernatant was removed and aliquoted into GC vial, followed by Speed Vacuum drying. Dried samples were sequentially derivatized with O-methoxyamine-HCL (2.5 h at 60 °C) and N,O-bis (trimethylsilyl) trifluoroacetaminde containing 10% trimethylchlorosilane (1.5 h at 80 °C). All derivatized cellular samples were analyzed on a HP 6890 GC coupled to a HP 5973 MSD under a full scan mode. Metabolomic profiling data were processed as previously (Lu et al., 2012). The data were first processed by principal component analysis (PCA), followed by partial least square-discriminant analysis (PLS-DA) to improve group separation and classify components with SIMCA-P + (U metrics). Hierarchical clustering analysis of the fold change of these identified molecular features between treatments and control was conducted. Following data acquisition, chromatograms were exported for peak alignment, retention time correction and statistical analysis. Three biological replicates per condition were analyzed for statistical significance. To profile individual metabolite differences between control and treatment groups, a 2-tailed Welch's t-test was used ($n = 3$, $p < 0.05$). Statistically significantly changed peaks ($p < 0.05$) were further identified by matching the spectra with NIST GC–MS library.

2.10. Statistical analysis

Three independent experiments were included in the analysis and each test condition was performed in triplicates or more. Values are

shown as the mean ± standard deviation from multiple experiments. Statistical significance was determined using one-way analysis of variance, among the groups followed by Tukey's multiple comparison test, with statistically significant at the cutoff level of $p < 0.05$ (GraphPad, Prism5, CA).

3. Results

3.1. Effect of BBP on cell viability in 3T3-L1 cells

In order to select non-cytotoxic doses of BBP in 3T3-L1 cells, cell viability was determined using the neutral red uptake assay. After 24 and 48 h of treatments, no significant effect on the cell viability of 3T3-L1 cells was observed at concentrations up to 100 μM of BBP. BBP at 200 μM showed a significant decrease of cell viability compared with the control ($p < 0.001$). Therefore, the concentrations below 100 μM of BBP were selected in the following experiments to examine the effect of BBP on the adipogenesis without obvious cytotoxicity (Fig. 2A).

3.2. BBP increases lipid droplet accumulation in 3T3-L1 cells

In order to elucidate the adipogenic properties of BBP, we applied Oil red O and Nile red staining assays to evaluate lipid droplets accumulation. As a positive control for the adipogenesis, cells were treated with M2 medium on day 0 to day 2, followed by M3 differentiation medium and M1 maturation medium. Tested compounds were included from the induction, differentiation and maturation stages until day 8. There was no DEX in the M2 medium when cells were treated with BBP or BPA. After 8 days of differentiation, 3T3-L1 preadipocytes underwent significant morphological changes from a spindle-like feature to a round shape, and accumulated intracellular lipids in the positive control. Cells in the positive control resulted in approximately 90% of the cells with positive lipid staining, indicating a higher degree of lipid accumulation in the maturated adipocyte. Both tested compound BBP and BPA significantly increased the lipid droplets at the concentration of 100 μM compared to the negative control (NC2) using Oil Red O staining (Fig. 2B). Quantitative measurement of intracellular triacylglycerides (TGs) using AdipoRed

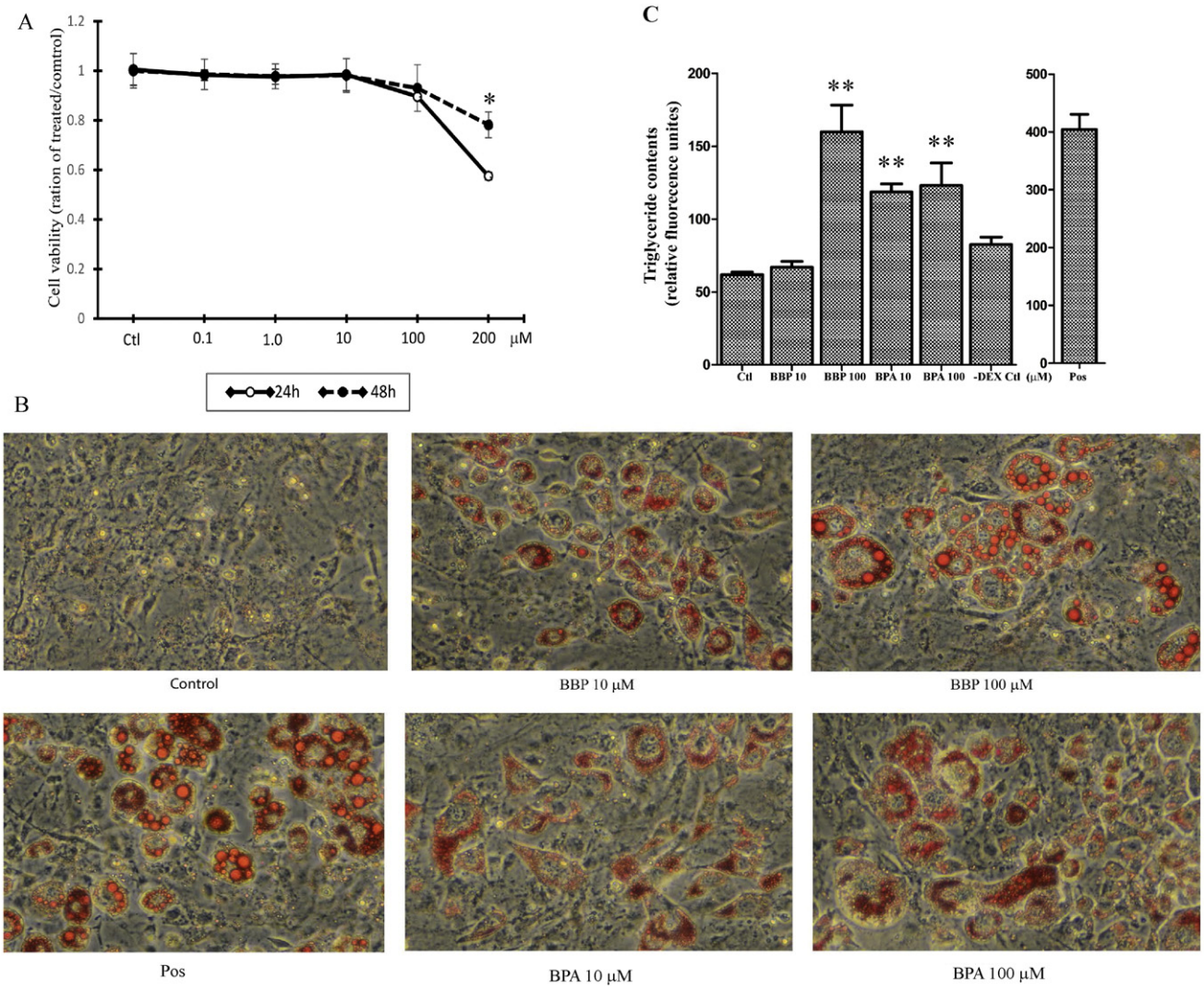

Fig. 2. Benzyl butyl phthalate (BBP) induced adipocyte differentiation in 3T3-L1. A. Cell viability (percentage of the control) was determined by Neutral red uptake assay after treatment with BBP for 24 or 48 h in 3T3-L1 cells. B. Effects of BBP or BPA on the lipid droplets accumulation using Oil Red O staining. The differentiation of 3T3-L1 preadipocytes was initiated 2 days after confluence in induction M2 medium containing DEX, IBMX and insulin (positive control, Pos). 3T3-L1 preadipocytes were exposed to BBP or BPA in M2 medium without DEX for two days, M3 medium for two days and M1 medium for maturation for four days. On day 8 of maturation, cells were stained with Oil Red O. C. Quantification of triglyceride content was conducted with AdipoRed assay in 3T3-L1 cells treated with BBP or BPA. Intensity of fluorescence was quantified with Gen 5 software (BioTek). The data shown represent the means ± SD of triplicates. The data was represented as three independent experiments. Statistical analysis was conducted by one-way ANOVA followed by Tukey's multiple comparison test. Asterisks * and ** represent statistical significance at $p < 0.05$, or $p < 0.001$, respectively, *versus* the NC2 control.

Assay (Fig. 2C) showed BBP treatment at 100 μM significantly increased the production of TGs, by 93.5% TG production compared to the NC2 control ($p < 0.01$), but not at a low dose of BBP (10 μM). BPA treatment significantly increased the lipid droplets accumulation by 43.5% and 48.8% at 10 and 100 μM, respectively, as compared with NC2 control ($p < 0.01$).

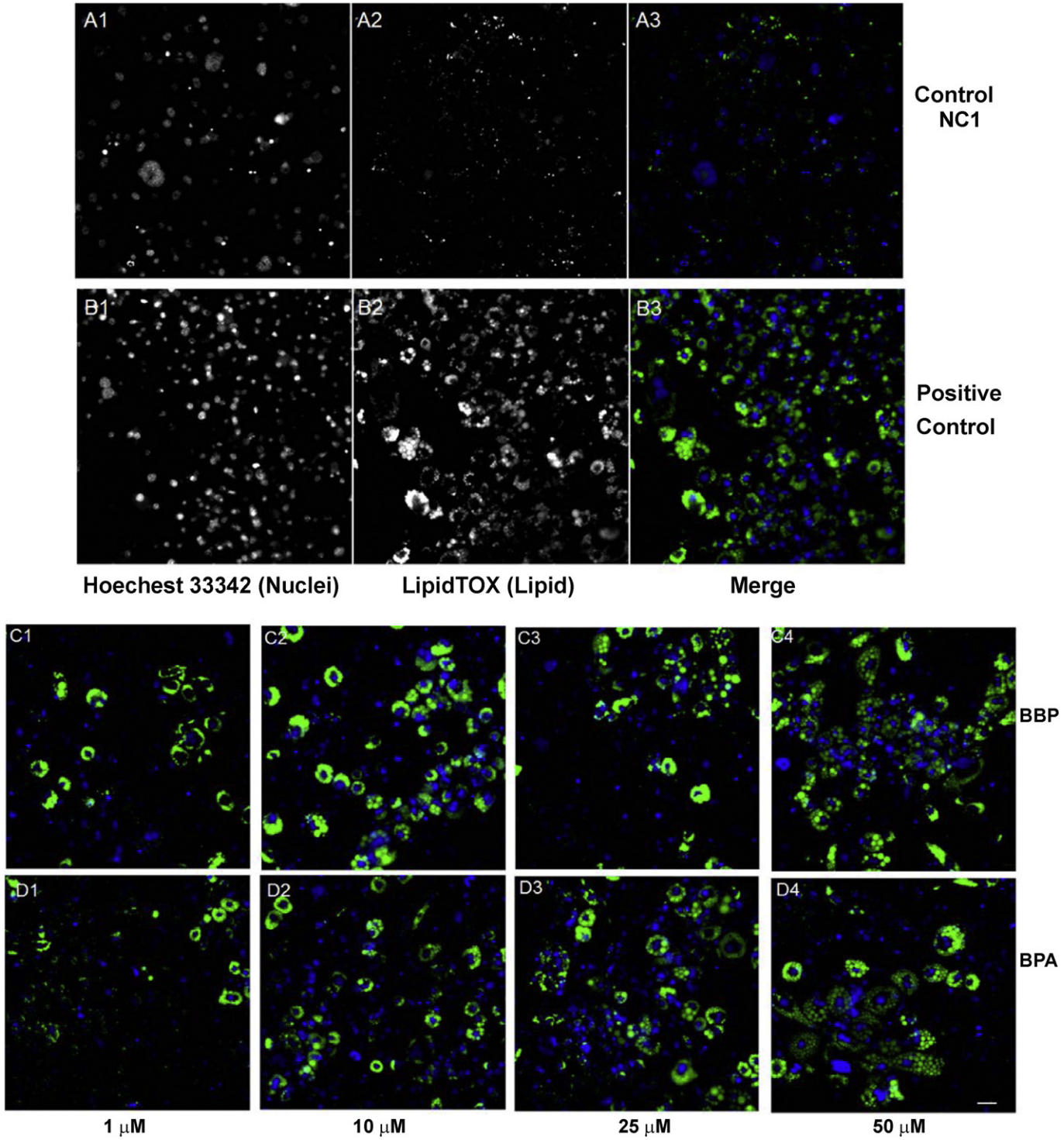

Fig. 3. Automated quantification of lipid droplets using High Content analysis in 3T3-L1 cells treated with BBP using Cellomics Arrayscan VTI. 3T3-L1 cells were inoculated in 96-well plates, and treated with BBP or BPA for eight days. The cells were stained with LipidTOX for neutral lipid (green) and Hoechst 33327 for nuclei (blue). Each image was automatically obtained with a 20× objective, and 49 fields/well. A1–3 and B1–3 demonstrates the two channel images from a negative control (NC1), and a positive control, C1–4 and D1–4 show the representative images of 3T3-L1 cells after treatment with BBP (C1:1 μM, C2:10 μM, C3: 25 μM, C4: 50 μM) or BPA (D1:1 μM, D2:10 μM, D3: 25 μM, D4: 50 μM). Each scale bar is 50 μm). E–H show the single cell-based quantification of lipid droplets in 3T3-L1 cells treated with BBP or BPA. The pixel intensity of the image for the lipid droplets were evaluated using the Target Activation BioApplication software, and then normalized to the number of cell nucleus. Each bar represents the mean ± SD ($n = 8$ replicates), and the experiments were repeated for three times). The cells treated with M2 induction medium without DEX was used as negative control (NC2). Statistical analysis was conducted by one-way ANOVA followed by Tukey's multiple comparison test. Asterisks **, ***, **** represent statistical significance at $p < 0.01$, $p < 0.001$, or $p < 0.0001$, respectively, *versus* the relative control.

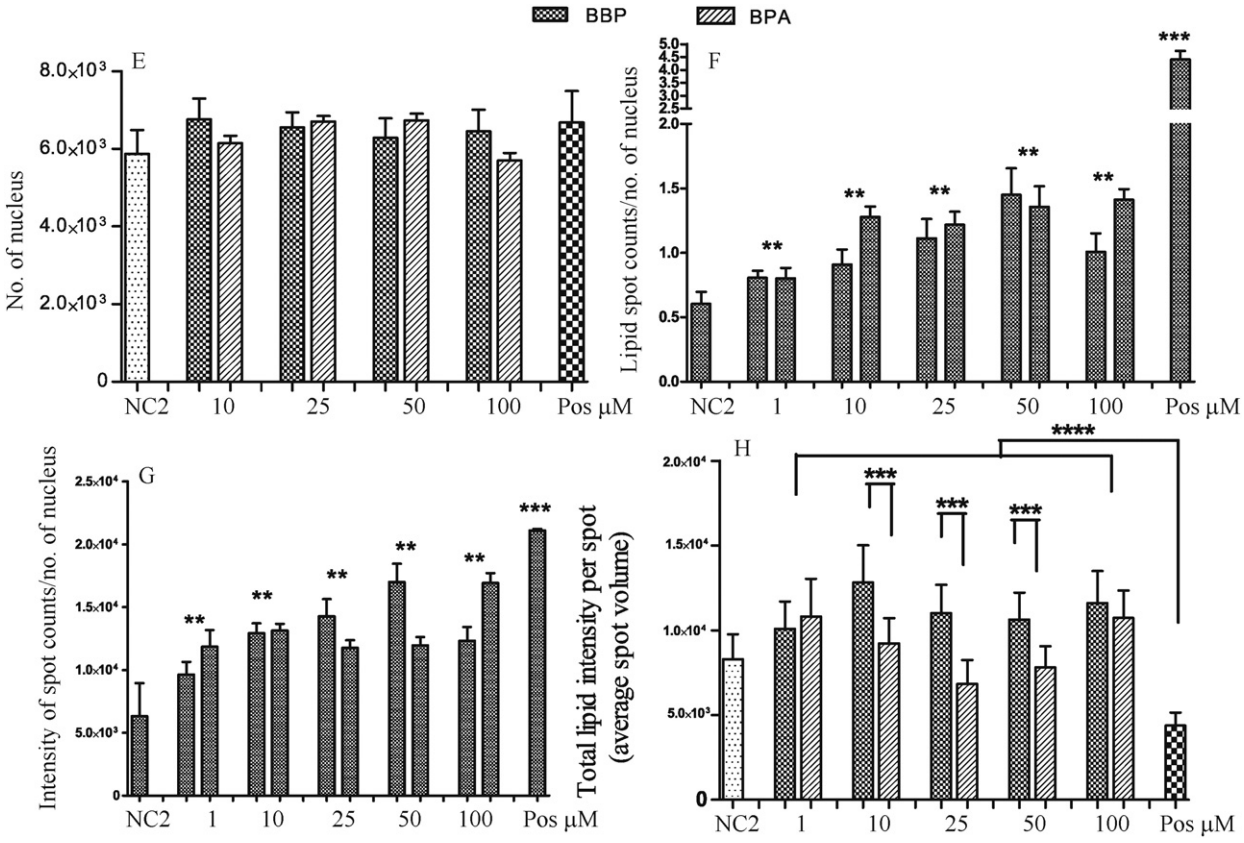

Fig. 3 (*continued*).

3.3. Cellomics based high-content analysis (HCA) of concentration-dependent effects of BBP and BPA on the neutral lipid accumulation

In order to develop more sensitive assay for the environmental obesogen screening, we applied a neutral lipid staining, LipidTOX, to investigate the adipogenic effects of BBP treatment using a cell-based Cellomics assay in a high throughput and high content format. We evaluated the effects of BBP on the lipid droplet accumulation in a wide range of concentrations (1, 10, 25 50 and 100 μM). A two-channel fluorescence analysis for the nuclear and lipid droplet (number of cells, size of lipid droplet and intensity of lipid droplet) was quantified. As shown in Fig. 3A 1–3, the control cells show evenly distributed lipid droplets with green fluorescent lipid-labeled, with size less than 0.05 μm. The lipid droplets in the positive control (Fig. 3B 1–3) show intensive neutral lipid droplet staining with LipidTOX green, indicating the hormone cocktail in the positive control efficiently achieved adipogenesis in 3T3-L1. Fig. 3C and D shows the representative photo of the lipid droplets staining after the treatments. In Fig. 3 C (1–4), the droplets size over 2 μm was observed at concentration (1 μM and above) of BBP. The number of droplets with lipid-labeled over 2 μm was much more abundant in the BBP treated cells compared to that of BBA treated group. There was no significant change of nuclear numbers after exposure to both BBP and BPA, indicating the concentrations used were within the non-cytotoxic concentrations range (Fig. 3E). Lipid spot counts and intensity of lipid spot counts per nucleus were significantly increased by both BPA and BBP treatments at concentrations of 1, 10, 25, 50 and 100 μM as compared to NC2 control (Fig. 3F and G). This single cell-based assay also showed that both BBP and BPA treatments increased lipid droplets size and lipid staining intensity with similar dose–response relationships, resulting in a "U shaped" dose response curves as shown in Fig. 3F and G. Both BBP and BPA treatments significantly increased lipid droplet size compared to that in the positive control. Most notably, BBP increased greater in size of lipid droplets compared to that of BPA treatment at the concentration of 10, 25, and 50 μM (Fig. 3H).

3.4. BBP induced dynamic changes of adipogenic regulatory genes

In order to examine the potential signaling pathways involved in the BBP induced adipogenesis, we measured the dynamic expression of adipogenic regulatory genes during three different stages of adipogenesis including induction (day 2), differentiation (day 4), and maturation (day 8). As shown in the Fig. 4, there were no significant changes of PPARγ and C/EBPα from day 2 to day 8 in the controls (NC1), while significant increased expressions of FABP4, AdipoQ, Adipsin and LPL from day 4 to day 8 in the controls were observed. As a positive control for the adipogenesis, the dynamic changes of all tested gene expression in the cells were observed with a dramatic 100 to 1000-fold increases in a time-dependent manner (Fig. 4H). PPARγ, C/EBPα, FASN and LPL expressions were significantly increased at the maturation stage of day 8, while FABP4, Adipsin and AdipoQ expression were significantly

Fig. 4. Dynamic gene expression changes in 3T3-L1 cells treated with BBP during adipogenesis. The differentiation of 3T3-L1 preadipocytes was initiated two days after confluence in induction M2 medium containing DEX, IBMX and insulin (positive control, Pos). 3T3-L1 preadipocytes were exposed to BBP in M2 medium without DEX for two days, M3 medium for two days and then M1 medium for a four day maturation. Total RNA was isolated during induction on day 2, differentiation on day 4 and maturation on day 8. The vehicle control (NC1) at day 2 served as controls. Changes in mRNA expression were evaluated by QRT-PCR and results are expressed as fold change of gene expression compared with the control after normalization with glyceraldehydes-3-phosphate dehydrogenase (GAPDH). Data are shown as the mean ± SD of triplicate ($n = 3$) from three independent experiments. Statistical analysis was conducted by one-way ANOVA followed by Tukey's multiple comparison test. Asterisks **, ***, **** represent statistical significance at $p < 0.01$, $p < 0.001$, or $p < 0.0001$, respectively, *versus* the NC1 control.

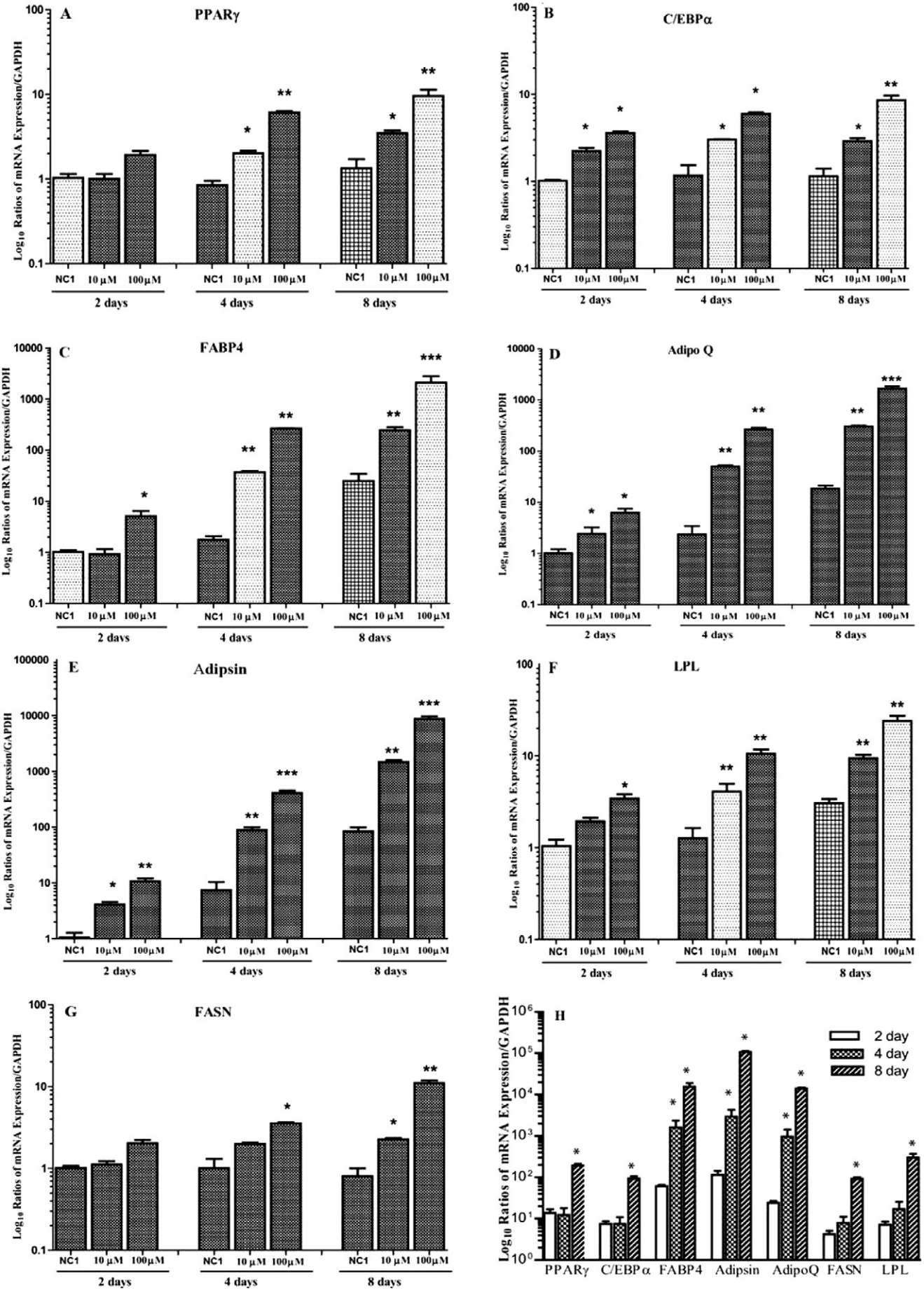
A
PPARγ
B
C/EBPα
C
FABP4
D
Adipo Q
E
Adipsin
F
LPL
G
FASN
H
Log10 Ratios of mRNA Expression/GAPDH
NC1
10 μM
100μM
2 days
4 days
8 days
2 day
4 day
8 day
PPARγ
C/EBPα
FABP4
Adipsin
AdipoQ
FASN
LPL

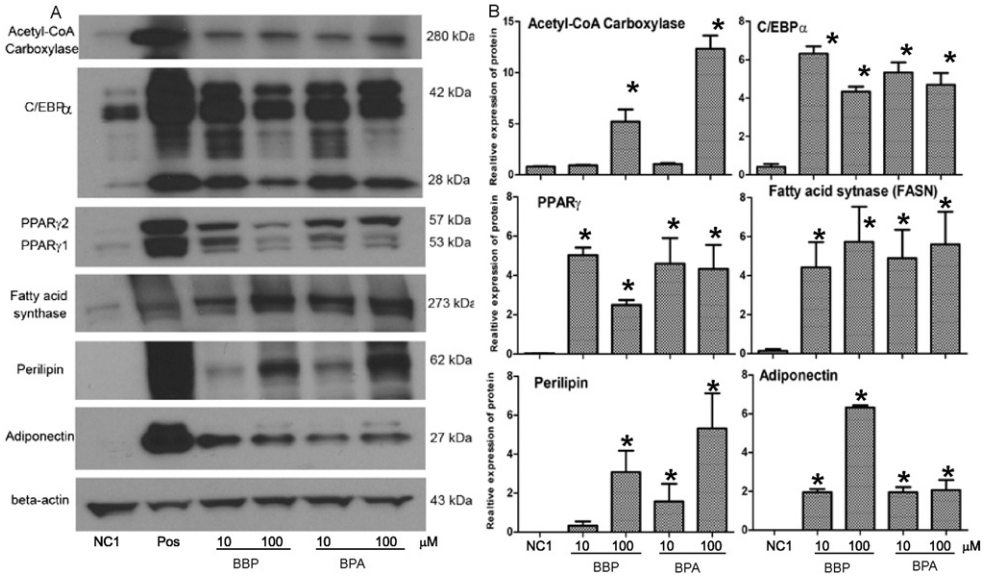

Fig. 5. BBP-induced adipogenic protein expressions in 3T3-L1 cells using Western blot analysis. The differentiation of 3T3-L1 preadipocytes was initiated two days after confluence in induction M2 medium containing DEX, IBMX and insulin (positive control, Pos). 3T3-L1 preadipocytes were exposed to BBP or BPA in M2 medium without DEX for two days, M3 medium for two days and M1 medium for maturation for four days. Cells were harvested on day 8, and proteins were extracted. Western blot analysis of PPAR-γ, C/EBP-α, acetyl-CoA Carboxylase (CoA), adiponectin, FABP4, fatty acid synthase (FASN), and perilipin was conducted. β-actin was used as an internal standard for the protein loading (A). The protein expression levels were quantified (B) using densitometric program Image J V1.49 (NIH), and quantitative data are the mean ± SD (n = 3), * $p < 0.05$.

increased at the stages of differentiation (day 4) and maturations (day 8) (Fig. 4H). BBP treatment induced dynamic and dose-dependent increase of the adipogenic transcriptional factors PPARγ during the differentiation (4 days) and maturation periods, but not at the early induction period (8 days, Fig. 4a). The gene expression of C/EBPα significantly increased in the early stage of induction (2 days), and continued to increase during differentiation (4 days) and maturation periods (8 days) in a dose dependent manner (Fig. 4b). BBP treatment dose-dependently up-regulated gene expression of adipocyte differentiation markers FABP4, AdipoQ, and Adipsin over 100-fold during the maturation period. Significant up-regulations of AdipoQ and Adipsin were observed at a low dose of 10 μM during the initial induction period, and continued to increase over the control by 100 and 500 folds until day 8 (Fig. 4d and e). Dose-dependent increase of FABP4 was observed during adipogenesis, with a significant increase at a low dose of 10 μM on days 4 and 8 (Fig. 4C). The enzyme that regulates adipogenesis, Lipoprotein lipase (LPL), was significantly increased in a dose and time dependent manner, statistically significant at 10 μM treatment on days 4 and 8, and at all stages at 100 μM of BBP (Fig. 4f). Another enzyme that regulates adipogenesis, Fatty acid synthase (FASN), was also significantly induced at 100 μM of BBP during the differentiation and maturation periods, and only significantly increased during the maturation (day 8) at 10 μM of BBP (Fig. 4g). Comparing the gene expression during the induction period of adipogenesis, only the genes, including C/EBPα, AdipoQ and Adipsin, were significantly induced by BBP at a low dose, the fold changes were 2.2, 2.5, and 4.1, respectively. All tested genes PPARγ, C/EBPα, FABP4, AdipoQ, Adipsin, LPL, and FASN, were significantly induced at the low dose of BBP treatments in both differentiation and maturation stages.

3.5. BBP exposure altered adipogenic proteins expression

The adipogenic efficacy of BBP was further validated during the differentiation process. Dose-dependent effects of BBP (10 and 100 μM) on the protein markers including acetyl-CoA carboxylase (ACC), C/EBPα, PPARγ, FASN, Adiponectin and perilipin were examined on day 8 (maturation period), as shown in Fig. 5A. In the positive control, significant increases of all these adipogenic protein markers were observed. Adipogenic marker C/EBPα, PPARγ, FASN, adiponectin, and perilipin were significantly increased at 10 or 100 μM of both BBP and BPA treatments, while ACC induction were observed at 100 μM of treatments (Fig. 5B). The expression levels of these markers at 10 μM of BBP were comparable to the levels observed at 10 μM BPA, a positive "obesogen".

3.6. BBP induced changes in metabolic profile during adipogenesis in 3T3-L1 cells

In order to explore the potential metabolites involved in the adipogenesis disrupted by BBP, we applied GC/MC based metabolomic tool to examine the metabolic profiles. Fig. 6A illustrated the changes of metabolic profiles in the 3T3-L1 cells under the treatments. In the positive control, 112 molecular features were identified to be statistically significant compared to the vehicle control, with 103 increased and 9 deceased, respectively (Fig. 6A). BBP treatment resulted in a significant change of 40 and 89 molecular features at concentrations of 10 and 100 μM, respectively (Fig. 6A). As shown in Fig. 6B, C, the (PCA and PLS-DA on these identified molecular features showed a clear separation between the control *versus* the positive control, BBP at 10 μM, or at 100 μM. The patterns of molecular features between the treatments of BBP (10 μM, 100 μM) and the positive control were significantly different from each other (Fig. 6D). Differential pattern between the low and high dose of BBP treatments was also observed (Fig. 6D). A number of metabolites with >1.5-fold change between the control and treatments were identified (Table 2). The structures of these metabolites were diverse, including lipid biosynthetic process, fatty acid metabolic process as well as steroid metabolic process. n-Butylamine, N,N-bis (trimethylsilyl) and Octadecanoic acid, trimethylsilyl ester were increased in the positive control and BBP treatments. Hexadecanoic acid, trimethylsilyl ester, Myo-Inositol, 1,2,3,4,5,6-hexakis-O-(trimethylsilyl)- and Silane, [(3β)-cholesta-5,24-dien-3-yloxy] trimethyl- were significantly increased in the positive control and 100 μM BBP. Silanol, trimethyl-, pyrophosphate (4:1) was significantly decreased in the group of 10 μM BBP while 19 fold increase was observed in the group of 100 μM BBP. (See Table 1.)

4. Discussion

As excess lipid droplet accumulation in cells is a hallmark of adipogenesis, a compound capable of inducing lipid accumulation could be considered as a potential obesogen. Based on this concept, we applied a neutral lipid staining combined with a High Content Cellomics analysis, and have shown that this new approach provided much more sensitivity and robustness compared to the conventional Oil red O and Nile red staining approaches. Moreover, we have further demonstrated that BBP significantly promotes adipogenesis through the up-regulation of adipogenic transcription factors, C/EBPα and PPARγ, and multiple adipogenic specific genes and proteins in a dose dependent and stage-specific manner. These results provide strong support for the application of this study for growing lists of potential environmental obesogens.

3T3-L1 preadipocytes are extensively used as an *in vitro* model for testing adipogenesis and recently proposed as an alternative *in vitro* model to screen environmental obesogens (Pereira-Fernandes et al., 2013; Pereira-Fernandes et al., 2014). In this study, the lipid droplet accumulation were qualitatively evaluated by Oil Red O staining, and the intracellular triacylglycerides (TGs) content was quantified using AdipoRed assay. As compared with these conventional approaches, we

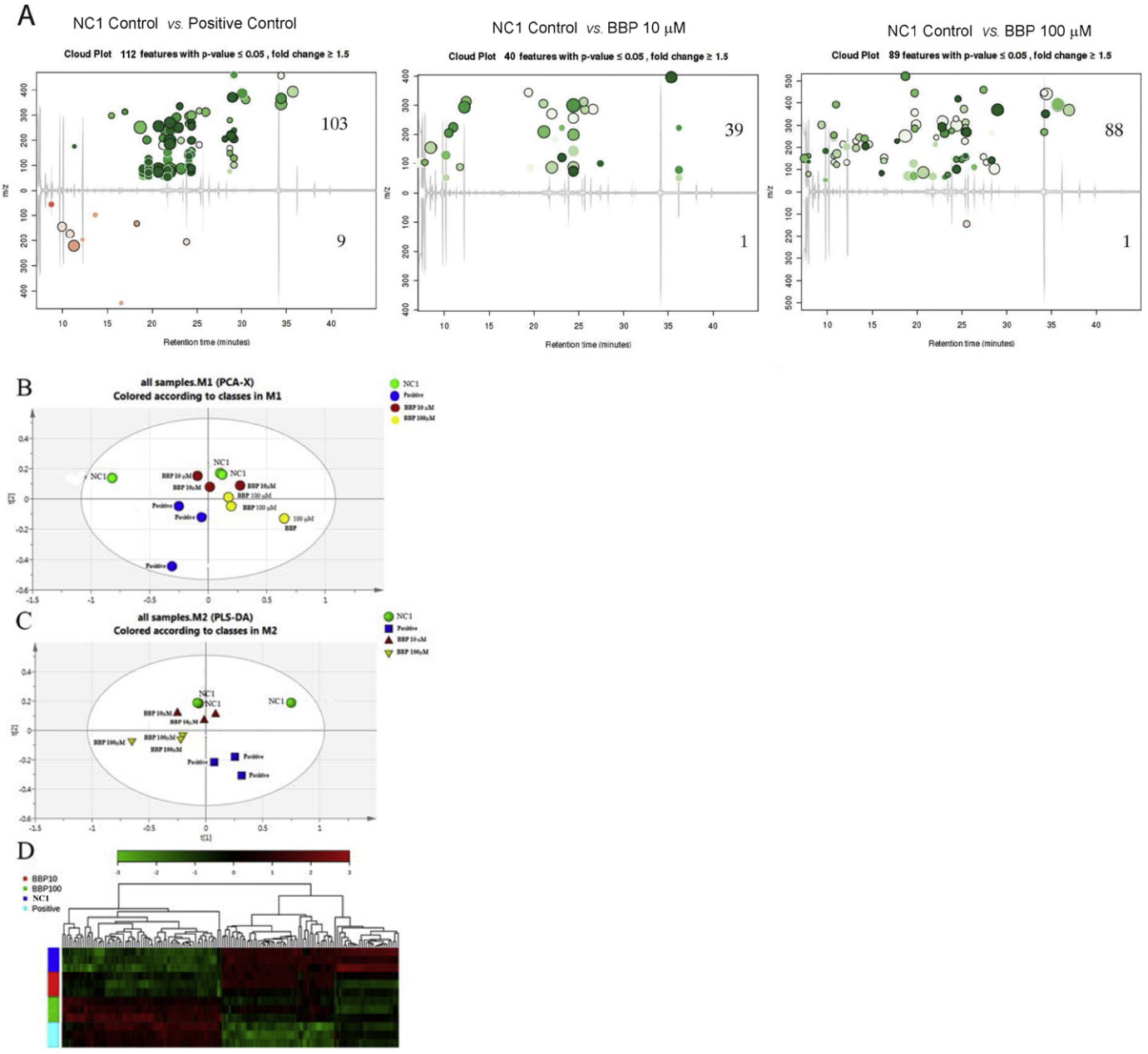

Fig. 6. BBP exposure altered metabolite profile in 3T3-L1 cells during adipogenesis. The differentiation of 3T3-L1 preadipocytes was initiated 2 days after confluence in M2 medium containing DEX, IBMX and insulin (positive control, Pos). 3T3-L1 preadipocytes were exposed to BBP at 10 μM, 100 μM (yellow) in M2 medium without DEX for two days, M3 medium for 2 days and M1 medium for maturation for 4 days. The DMSO vehicle control was indicated as (NC1, green). (A) Significant changes in metabolic profile of 3T3-L1 cells during the adipogenesis, with 112, 40 and 90 molecular features being significantly changed in the positive control, BBP at 10 μM and 100 μM, respectively, as compared with controls (fold change >1.5 and $p < 0.05$, $n = 3$). (B) The principle component analysis (PCA, B) and partial least-squares discriminant analysis (PLS-DA, C) models were constructed using molecular features with 1.5-fold changes ($p < 0.05$, $n = 3$), showing a clear separation of groups among positive control, BBP treatment at 10 μM and 100 μM. (D). The hierarchical clustering map constructed using molecular features with 1.5-fold changes ($p < 0.05$, $n = 3$) shows a consistent clustering pattern within individual groups.

Table 1
Oligonucleotide primer sequences for real-time RT-PCR.

Gene name (accession no.)	Forward primer (5′–3′)	Reverse primer (5′–3′)	Product size (bp)
PPARγ NM_133249	TCCTGTAAAAGCCCGGAGTAT	GCTCTGGTAGGGGCAGTGA	174
C/EBPα NM_007678	CAAGAACAGCAACGAGTACCG	GTCACTGGTCAACTCCAGCAC	124
FABP4 NM_024406	AAGGTGAAGAGCATCATAACCCT	TCACGCCTTTCATAACACATTCC	133
LPL NM_008509	GGGAGTTTGGCTCCAGAGTTT	TGTGTCTTCAGGGGTCCTTAG	155
FASN NM_007988	GGAGGTGGTGATAGCCGGTAT	TGGGTAATCCATAGAGCCCAG	140
AdipoQ NM_009605	TGTTCCTCTTAATCCTGCCCA	CCAACCTGCACAAGTTCCCTT	140
ADIPSIN NM_013459	CATGCTCGGCCCTACATGG	CACAGAGTCGTCATCCGTCAC	129

applied a cell-based LipidTOX HCA assay to quantify the lipid droplet accumulation. Adipogenesis is a multiple stage process, and the spontaneous differentiation of 3T3-L1 is regulated by a cascade of transcriptional events. Currently, there is no consensus protocol on the "exposure scenarios" to evaluate the obesogenic effects using an *in vitro* model. Two exposure scenarios, including "single-compound treatment" and "insulin supplemented exposure", were reported to examine the obesogenic effect (Pereira-Fernandes et al., 2013). In the single-compound treatment scenario, BBP and di-iso-butyl phthalate (DBP) were revealed as strong and weak obesogen, respectively (Pereira-Fernandes et al.,

Table 2
Metabolites identified in GC/MC analysis. The differentiation of 3T3-L1 preadipocytes was initiated 2 days after confluence in induction M2 medium containing DEX, IBMX and insulin (positive control). 3T3-L1 preadipocytes were exposed to BBP at 10 μM and 100 μM in M2 medium without DEX for two days, M3 medium for two days of differentiation, and M1 medium for 4 days of maturation. DEX was included in the induction M2 medium, followed by M3 and M1, which was set as a positive control. The DMSO vehicle control was indicated as NC1. Cellular samples were analyzed on a HP 6890 GC coupled to a HP 5973 MSD under a full scan mode. Following data acquisition, chromatograms were exported for peak alignment, retention time correction and statistical analysis. Statistically significantly changed peaks ($n = 3$, $p < 0.05$) were further identified by matching the spectra with NIST GC–MS library. 1, 2 or 3 represents metabolites significantly changed in all groups, BBP treatments at both 10 and 100 μM groups, and positive control and BBP at 100 μM groups, respectively.

Metabolites identified	RT (min)	m/z	MQ (%)	Fold change at each m/z	*
Control vs. positive control					
Tris(trimethylsilyl)carbamate	11.0	175.1/132.1	95.1	1.8/1.98	
n-Butylamine, N,N-bis(trimethylsilyl)	11.3	175.1/132.2	71.8	1.8/2.0	1
Decanedioic acid, bis(tert-butyldimethylsilyl) ester	14.5	298.1	62.7	2.8	
Phosphoric acid, bis(trimethylsilyl) 2,3-bis[(trimethylsilyl)oxy]propyl ester	19.7	85.2/57.2	73.5	4.4/3.7	
Palmitelaidic acid, trimethylsilyl ester	23.2	199.2	53.9	3.0	
Hexadecanoic acid, trimethylsilyl ester	23.4	199.2/87.1	97.3	3.0/11.7	3
Myo-inositol, 1,2,3,4,5,6-hexakis-O-(trimethylsilyl)	23.8	111.2/151.2/296.3	83.3	3.4/3.6/4.5	3
Heptadecanoic acid, trimethylsilyl ester	24.6	75.1	69	1.6	
Octadecanoic acid, trimethylsilyl ester	25.7	181.1	98.4	2.2	1
Hexadecanoic acid, 2,3-bis[(trimethylsilyl)oxy]propyl ester	29.1	149.1/101.1/205.2/129.1/239.3/460.4/371.4	89.1	2.1/2.5/4.1/2.7/2.8/3.5/3.5	
Silane, [(3β)-cholesta-5,24-dien-3-yloxy]trimethyl-	34.4	457.5/344.3/366.4	83	2.6/16.5/10.6	3
Glyoxylic oxime acid, bis(trimethylsilyl)-	9.9	144.1	49.8	−5.3	
L-Valine, N-(trimethylsilyl)-, trimethylsilyl ester	11.3	220.2	53.7	−11.0	
Silanol, trimethyl-, phosphate (3:1)	12.2	196.05	95.9	−1.7	
Control vs. BBP 10 μM					
Ethylbis(trimethylsilyl)amine	7.6	103.2/104.1	74.9	2.7/1.5	
Glycine, N-(trimethylsilyl)-, trimethylsilyl ester	9.9	52.2	87	1.8	
n-Butylamine, N,N-bis(trimethylsilyl)	11.3	88.1	60.5	1.6	1
3,6,9-Trioxa-2,10-disilaundecane, 2,2,10,10-tetramethyl-	11.7	88.1	70.1	1.6	
Silanol, trimethyl-, phosphate (3:1)	12.2	293.2	95.3	3.7	
Octadecanoic acid, trimethylsilyl ester	25.7	311.3/72.2/285.3	97.4	2.2/2.1/2	1
Silanol, trimethyl-, pyrophosphate (4:1)	18.3	132.1	62.4	−1.4	2
Control vs. BBP 100 μM					
Ethylbis(trimethylsilyl)amine	7.5	151.1/178.1	69.3/82.6	3.9/1.2	
Cystathionine, bis(triemthylsilyl) ester	9.3	301.2	60.5	3.1	
Phosphoric acid, bis(trimethylsilyl)monomethyl ester	10.7	133.1/242.1/241.1/243.1/163.1/256.1	92.9	1.9/2.3/1.9/1.9/1.9	
Tris(trimethylsilyl)carbamate	11.1	133.1	94.6	1.9	
n-Butylamine, N,N-bis(trimethylsilyl)	11.3	172.1	59.7	3.6	1
Decanedioic acid, bis(tert-butyldimethylsilyl) ester	14.4	205.1	58.1	2.8	
L-Proline, 5-oxo-1-(trimethylsilyl)-, trimethylsilyl ester	16.3	140.1/157.1/154.1	87.6	2.1/2.2/2.8	
Silanol, trimethyl-, pyrophosphate (4:1)	18.3	251.2	96.7	19.3	2
Phosphoric acid, 2-[bis(trimethylsilyl)amino]ethyl bis(trimethylsilyl) ester	20.0	302.1	88	6.4	
Hexadecanoic acid, trimethylsilyl ester	23.4	77.1	96.8	1.8	3
Myo-Inositol, 1,2,3,4,5,6-hexakis-O-(trimethylsilyl)-	23.8	275.2	83.5	1.9	3
Octadecanoic acid, trimethylsilyl ester	25.7	228.2/269.2	97.2	2.6/4.9	1
Cholesterol trimethylsilyl ether	34.2	269.3/445.4	81.6	2.4/2.6	
Silane, [(3β)-cholesta-5,24-dien-3-yloxy]trimethyl-	34.4	351.4/441.4	71.1	3.5/12.5	3

2014). However, in the insulin supplemented exposure scenarios, both BBP and DBP were shown more potency in promoting adipocyte differentiation. A strong effect of DBP on adipocyte differentiation was observed in the insulin-compound co-treatment experiments, but not in the single-compound treatment. Therefore, the "exposure scenarios" toward the differentiation of adipocyte will significantly affect the sensitivity in the identification of the obesogenic effects of the compound. In the current study, we exposed BBP or BPA during the entire adipogenesis process, without adding DEX in the M2 medium during the first two day period as compared to the positive control. DEX is a synthetic glucocorticoid and has been used as a critical component of differentiation medium for preadipocyte differentiation. DEX removal significantly decreased the adipocyte differentiation (Fig. 2C), as the lipid droplets were barely detected. We found from the current treatment protocol that there was a dose-dependent effect of BBP or BPA on the lipid droplet accumulation with multiple parameters tested. Since the differentiation of adipocyte involves in multiple steps and several signaling pathways, additional examinations on the "exposure scenario" will be very crucial to accurately decipher the molecular mechanisms for the identification of potential obesogen.

In a recent transcriptomic study, BBP was found to exhibit a similar transcription pattern associated with adipocyte differentiation as BPA (Pereira-Fernandes et al., 2014). BPA was found to play an important role in lipid metabolism and accumulation during development and adulthood by disrupting adipogenesis and lipogenic signaling pathways, and was found to be closely associated with the development of obesity and diabetes in rodent and human mode (Bhandari et al., 2013; Boucher et al., 2014; Masuno et al., 2005; Picard et al., 2001). We included BPA as an experimental positive control, and found that BPA promotes adipogenesis as evidenced by the accumulation of lipid droplets and induction of multiple adipogenic markers, which is consistent with previous findings (Boucher et al., 2014). Our current study confirmed that BBP exposure resulted in potent adipogenic effect with a similar extent of BPA exposure in 3T3-L1 cells.

Cellomics based HCS with LipidTOX staining showed that both BBP and BPA exposure resulted in "U shaped" dose-dependent of lipid droplet accumulation. As compared to the vehicle control, BBP was found to significantly promote lipid accumulation arranging from 1 μM to 50 μM, which is approximately 50 times more sensitive than Oil Red O staining as well as the Nile red-based AdipoRed assay. As shown in the Fig. 3, Cellomics based HCS analysis provided multiple cellular parameters, including the number of nucleus, total intensity of the lipid droplets per each well, total counts of lipid spots, and average spot volume (total lipid intensity per spot). Therefore, it is obvious advantages to using LipidTox HCA analysis as a high throughput screen platform for environmental obesogen screening. As shown in Fig. 3C–G, the dose for adipogenic effects of BPA or BBP were far less than those doses causing cytotoxic effects. Interestingly, the low dose of BBP (1 μM) could potentially affect the adipogenesis, while the higher dose of BBP may have adverse health effect on other organ systems, such as the reproductive system. In our previous study, phthalates, including BBP (above 100 μM), were found to have anti-androgenic effects on the testicular cells through the changes in expression of steroidogenic related genes (Yu et al., 2009). It implicated that phthalates like BBP may potentiate the development of obesity at doses far below the levels previously determined to be toxicity to the male reproductive system. In additional, previous findings suggest that the size and number of the lipid droplets within adipocytes could affect the secretion of free fatty acids, which is associated with the development of insulin resistance (Kubota et al., 1999). In the current study, we have found that BBP significantly increased greater in size of lipid droplet as compared with that of BPA. The differential effects between BBP and BPA suggested divergent mechanisms of action between BBP and BPA, and these mechanisms may be chemical structure dependent.

Two major transcriptional factors PPARγ and C/EBPα are found to be involved in the regulation of adipogenesis (Madsen et al., 2014; Ntambi and Young-Cheul, 2000; Rosen, 2005). BBP induced differential dynamic changes of these two transcriptional factors, with a significant higher expression of C/EBPα than PPARγ at the early induction stage. PPARγ acts as regulator for adipocyte differentiation and lipid metabolism, and proposed to be a direct link between PPARγ agonists and obesogens (Wang et al., 2010). However, PPARγ receptor activation is neither a requirement nor an assurance for adipogenesis, indicating the importance of other mechanisms such as glucocorticoid receptor (GR) activation (Pereira-Fernandes et al., 2013; Taxvig et al., 2012). C/EBPα has been reported to be specifically involved in activating the gene program in driving insulin-stimulated glucose uptake (Tamori et al., 2002). In current study, BBP was treated in 3T3-l1 cells throughout the whole course of differentiation period in the absence of DEX, an agonist of glucocorticoid receptor (GR), in order to elucidate glucocorticoid-mediated effect on lipid metabolism. We have found that BBP significantly induced adipogenesis in the absence of DEX, suggesting a potential ability of BBP agonists to GR.

We have demonstrated that BBP exposure altered the metabolomic profiles. Multiple fatty acid associated pathways, such as decanedioic acid, butylamine, and octadecanoic acid, were upregulated in BBP treatments (10 and 100 μM). Decanedioic acid has been associated with the function of glycogen storage (Bergoffen et al., 1993). Butylamine, known as agonists of the glucocorticoid receptor (GR) signaling pathway (Huang et al., 2011), links to the function of metabolic process. Octadecanoic acid, a saturated fatty acid, has been clearly associated with the development of obesity (Caron-Jobin et al., 2012). In the high dose of BBP treatment, additional multiple metabolites such as cholesterol, phosphoric acid, silane and proline, were shown to be significantly up-regulated. In consistent with the observation of the lipid droplet accumulation and stage-specific activation of adipogenic genes, GC/MS based metabolomic analysis represents a critical step further toward understanding how BBP exposure promotes the adipogenesis. We found the unique molecular metabolite silanol, trimethyl, pyrophosphate with an opposite direction of changes at the low and high BBP treatments. Interestingly, BBP up-regulated pyrophosphate, a mevalonate metabolite, can activate PPARγ as an agonist during adipocyte differentiation (Goto et al., 2011). These findings suggest that high dose of BBP may function as an endogenous PPARγ ligand and regulate adipocyte differentiation. Future studies are warranted to delineate the mechanistic basis of these metabolites and possibly lead to discovery of molecular metabolite biomarker for environmentally induced obesity. The information generated by metabolomic analysis provides us with increased knowledge on how the metabolic signaling pathways are perturbed after environmental chemicals exposure (Xie et al., 2012). The differential metabolic patterns using metabolomics showed an invaluable tool for evaluation of metabolic activities, which may contribute to candidate biomarker discovery for obesity.

In summary, our current study provides evidence that BBP treatment promoted lipid droplet accumulation and induced adipogenesis through the alterations of dynamic transcriptional factors and their adipogenic differentiation markers. Further in-depth *in vivo* research will be crucial to fully comprehend its role in the development of obesity as well as the mechanism of action. Also, our current study established a Cellomics-based high-throughput screening protocol, which will be invaluable for the identification of environmental obesogen and ultimately for the prevention of chemical-induced obesity.

Acknowledgments

This work was supported by CDC R21 OH 010473, Alternatives Research & Development Foundation (ARDF) and the University of Georgia Startup Research funding (1025AR715005). We appreciate Ms. Adrianne Marguerite Smith for proofreading the manuscript.

References

Agas, D., Sabbieti, M.G., Capacchietti, M., Materazzi, S., Menghi, G., Materazzi, G., Hurley, M.M., Marchetti, L., 2007. Benzyl butyl phthalate influences actin distribution and cell proliferation in rat Py1a osteoblasts. J. Cell. Biochem. 101, 543–551.

Allender, S., Rayner, M., 2007. The burden of overweight and obesity-related ill health in the UK. Obes. Rev. 8, 467–473.

Baillie-Hamilton, P.F., 2002. Chemical toxins: a hypothesis to explain the global obesity epidemic. J. Altern. Complement. Med. 8, 185–192.

Bergoffen, J., Kaplan, P., Hale, D.E., Bennett, M.J., Berry, G.T., 1993. Marked elevation of urinary 3-hydroxydecanedioic acid in a malnourished infant with glycogen storage disease, mimicking long-chain L-3-hydroxyacyl-CoA dehydrogenase deficiency. J. Inherit. Metab. Dis. 16, 851–856.

Bhandari, R., Xiao, J., Shankar, A., 2013. Urinary bisphenol A and obesity in U.S. children. Am. J. Epidemiol. 177, 1263–1270.

Boucher, J.G., Boudreau, A., Atlas, E., 2014. Bisphenol A induces differentiation of human preadipocytes in the absence of glucocorticoid and is inhibited by an estrogen-receptor antagonist. Nutr. Diabetes 4, e102.

Brady, M.J., Kartha, P.M., Aysola, A.A., Saltiel, A.R., 1999. The role of glucose metabolites in the activation and translocation of glycogen synthase by insulin in 3T3-L1 adipocytes. J. Biol. Chem. 274, 27497–27504.

Buser, M.C., Murray, H.E., Scinicariello, F., 2014. Age and sex differences in childhood and adulthood obesity association with phthalates: analyses of NHANES 2007–2010. Int. J. Hyg. Environ. Health 217, 687–694.

Caron-Jobin, M., Mauvoisin, D., Michaud, A., Veilleux, A., Noel, S., Fortier, M.P., Julien, P., Tchernof, A., Mounier, C., 2012. Stearic acid content of abdominal adipose tissues in obese women. Nutr. Diabetes 2, e23.

Choi, J., Eom, J., Kim, J., Lee, S., Kim, Y., 2014. Association between some endocrine-disrupting chemicals and childhood obesity in biological samples of young girls: a cross-sectional study. Environ. Toxicol. Pharmacol. 38, 51–57.

Desvergne, B., Feige, J.N., Casals-Casas, C., 2009. PPAR-mediated activity of phthalates: a link to the obesity epidemic? Mol. Cell. Endocrinol. 304, 43–48.

Foster, P.M., 2006. Disruption of reproductive development in male rat offspring following in utero exposure to phthalate esters. Int. J. Androl. 29, 140–147 discussion 181-145.

Frederiksen, H., Skakkebaek, N.E., Andersson, A.M., 2007. Metabolism of phthalates in humans. Mol. Nutr. Food Res. 51, 899–911.

Goto, T., Nagai, H., Egawa, K., Kim, Y.I., Kato, S., Taimatsu, A., Sakamoto, T., Ebisu, S., Hohsaka, T., Miyagawa, H., Murakami, S., Takahashi, N., Kawada, T., 2011. Farnesyl pyrophosphate regulates adipocyte functions as an endogenous PPARgamma agonist. Biochem. J. 438, 111–119.

Gray Jr., L.E., Ostby, J., Furr, J., Price, M., Veeramachaneni, D.N., Parks, L., 2000. Perinatal exposure to the phthalates DEHP, BBP, and DINP, but not DEP, DMP, or DOTP, alters sexual differentiation of the male rat. Toxicol. Sci. 58, 350–365.

Grun, F., Blumberg, B., 2007. Perturbed nuclear receptor signaling by environmental obesogens as emerging factors in the obesity crisis. Rev. Endocr. Metab. Disord. 8, 161–171.

Hao, C., Cheng, X., Xia, H., Ma, X., 2012. The endocrine disruptor mono-(2-ethylhexyl) phthalate promotes adipocyte differentiation and induces obesity in mice. Biosci. Rep. 32, 619–629.

Harris, C.A., Henttu, P., Parker, M.G., Sumpter, J.P., 1997. The estrogenic activity of phthalate esters in vitro. Environ. Health Perspect. 105, 802–811.

Hatch, E.E., Nelson, J.W., Qureshi, M.M., Weinberg, J., Moore, L.L., Singer, M., Webster, T.F., 2008. Association of urinary phthalate metabolite concentrations with body mass index and waist circumference: a cross-sectional study of NHANES data, 1999-2002. Environ. Heal. 7, 27.

Heudorf, U., Mersch-Sundermann, V., Angerer, J., 2007. Phthalates: toxicology and exposure. Int. J. Hyg. Environ. Health 210, 623–634.

Hossain, P., Kawar, B., El Nahas, M., 2007. Obesity and diabetes in the developing world—a growing challenge. N. Engl. J. Med. 356, 213–215.

Huang, R., Xia, M., Cho, M.H., Sakamuru, S., Shinn, P., Houck, K.A., Dix, D.J., Judson, R.S., Witt, K.L., Kavlock, R.J., Tice, R.R., Austin, C.P., 2011. Chemical genomics profiling of environmental chemical modulation of human nuclear receptors. Environ. Health Perspect. 119, 1142–1148.

Hurst, C.H., Waxman, D.J., 2003. Activation of PPARalpha and PPARgamma by environmental phthalate monoesters. Toxicol. Sci. 74, 297–308.

Hursting, S.D., Dunlap, S.M., 2012. Obesity, metabolic dysregulation, and cancer: a growing concern and an inflammatory (and microenvironmental) issue. Ann. N. Y. Acad. Sci. 1271, 82–87.

Janesick, A., Blumberg, B., 2011. Endocrine disrupting chemicals and the developmental programming of adipogenesis and obesity. Birth Defects Res. C Embryo Today 93, 34–50.

Kim, S.H., Park, M.J., 2014. Phthalate exposure and childhood obesity. Ann. Pediatr. Endocrinol. Metab. 19, 69–75.

Koch, H.M., Preuss, R., Angerer, J., 2006. Di(2-ethylhexyl)phthalate (DEHP): human metabolism and internal exposure — an update and latest results. Int. J. Androl. 29, 155–165 (discussion 181-155).

Kubota, N., Terauchi, Y., Miki, H., Tamemoto, H., Yamauchi, T., Komeda, K., Satoh, S., Nakano, R., Ishii, C., Sugiyama, T., Eto, K., Tsubamoto, Y., Okuno, A., Murakami, K., Sekihara, H., Hasegawa, G., Naito, M., Toyoshima, Y., Tanaka, S., Shiota, K., Kitamura, T., Fujita, T., Ezaki, O., Aizawa, S., Kadowaki, T., et al., 1999. PPAR gamma mediates high-fat diet-induced adipocyte hypertrophy and insulin resistance. Mol. Cell 4, 597–609.

Latini, G., Del Vecchio, A., Massaro, M., Verrotti, A., C, D.E.F., 2006. In utero exposure to phthalates and fetal development. Curr. Med. Chem. 13, 2527–2534.

Lind, P.M., Roos, V., Ronn, M., Johansson, L., Ahlstrom, H., Kullberg, J., Lind, L., 2012. Serum concentrations of phthalate metabolites are related to abdominal fat distribution two years later in elderly women. Environ. Heal. 11, 21.

Lu, K., Knutson, C.G., Wishnok, J.S., Fox, J.G., Tannenbaum, S.R., 2012. Serum metabolomics in a *Helicobacter hepaticus* mouse model of inflammatory bowel disease reveal important changes in the microbiome, serum peptides, and intermediary metabolism. J. Proteome Res. 11, 4916–4926.

Madsen, L., Petersen, R.K., Sorensen, M.B., Jorgensen, C., Hallenborg, P., Pridal, L., Fleckner, J., Amri, E.Z., Krieg, P., Furstenberger, G., Berge, R.K., Kristiansen, K., 2003. Adipocyte differentiation of 3T3-L1 preadipocytes is dependent on lipoxygenase activity during the initial stages of the differentiation process. Biochem. J. 375, 539–549.

Madsen, M.S., Siersbaek, R., Boergesen, M., Nielsen, R., Mandrup, S., 2014. Peroxisome proliferator-activated receptor gamma and C/EBPalpha synergistically activate key metabolic adipocyte genes by assisted loading. Mol. Cell. Biol. 34, 939–954.

Masuno, H., Iwanami, J., Kidani, T., Sakayama, K., Honda, K., 2005. Bisphenol a accelerates terminal differentiation of 3T3-L1 cells into adipocytes through the phosphatidylinositol 3-kinase pathway. Toxicol. Sci. 84, 319–327.

McTigue, K.M., Chang, Y.F., Eaton, C., Garcia, L., Johnson, K.C., Lewis, C.E., Liu, S., Mackey, R.H., Robinson, J., Rosal, M.C., Snetselaar, L., Valoski, A., Kuller, L.H., 2014. Severe obesity, heart disease, and death among white, African American, and Hispanic postmenopausal women. Obesity (Silver Spring) 22, 801–810.

Nativelle, C., Picard, K., Valentin, I., Lhuguenot, J.C., Chagnon, M.C., 1999. Metabolism of n-butyl benzyl phthalate in the female Wistar rat. Identification of new metabolites. Food Chem. Toxicol. 37, 905–917.

Newbold, R.R., Padilla-Banks, E., Jefferson, W.N., 2009. Environmental estrogens and obesity. Mol. Cell. Endocrinol. 304, 84–89.

Ntambi, J.M., Young-Cheul, K., 2000. Adipocyte differentiation and gene expression. J. Nutr. 130, 3122S–3126S.

OECD, 2012. Detailed Review Paper on the State of the Science on Novel in vitro and in vivo Screening and Testing Methods and Endpoints for Evaluating Endocrine Disruptors. No. 178. (Available at) http://search.oecd.org/officialdocuments/displaydocumentpdf/?cote=env/jm/mono(2012)23&doclanguage = en (Accessed Nov, 2015).

Pe reira-Fernandes, A., Demaegdt, H., Vandermeiren, K., Hectors, T.L., Jorens, P.G., Blust, R., Vanparys, C., 2013. Evaluation of a screening system for obesogenic compounds: screening of endocrine disrupting compounds and evaluation of the PPAR dependency of the effect. PLoS ONE 8, e77481.

Pereira-Fernandes, A., Vanparys, C., Vergauwen, L., Knapen, D., Jorens, P.G., Blust, R., 2014. Toxicogenomics in the 3T3-L1 cell line, a new approach for screening of obesogenic compounds. Toxicol. Sci. 140, 352–363.

Picard, K., Lhuguenot, J.C., Lavier-Canivenc, M.C., Chagnon, M.C., 2001. Estrogenic activity and metabolism of n-butyl benzyl phthalate in vitro: identification of the active molecule(s). Toxicol. Appl. Pharmacol. 172, 108–118.

Piersma, A.H., Verhoef, A., te Biesebeek, J.D., Pieters, M.N., Slob, W., 2000. Developmental toxicity of butyl benzyl phthalate in the rat using a multiple dose study design. Reprod. Toxicol. 14, 417–425.

Reddy, B.S., Rozati, R., Reddy, B.V., Raman, N.V., 2006. Association of phthalate esters with endometriosis in Indian women. BJOG 113, 515–520.

Repetto, G., del Peso, A., Zurita, J.L., 2008. Neutral red uptake assay for the estimation of cell viability/cytotoxicity. Nat. Protoc. 3, 1125–1131.

Rosen, E.D., 2005. The transcriptional basis of adipocyte development. Prostaglandins Leukot. Essent. Fat. Acids 73, 31–34.

Shin, I.S., Lee, M.Y., Cho, E.S., Choi, E.Y., Son, H.Y., Lee, K.Y., 2014. Effects of maternal exposure to di(2-ethylhexyl)phthalate (DEHP) during pregnancy on susceptibility to neonatal asthma. Toxicol. Appl. Pharmacol. 274, 402–407.

Shultz, V.D., Phillips, S., Sar, M., Foster, P.M., Gaido, K.W., 2001. Altered gene profiles in fetal rat testes after in utero exposure to di(n-butyl) phthalate. Toxicol. Sci. 64, 233–242.

Song, Y., Hauser, R., Hu, F.B., Franke, A.A., Liu, S., Sun, Q., 2014. Urinary concentrations of bisphenol A and phthalate metabolites and weight change: a prospective investigation in US women. Int. J. Obes.

Stahlhut, R.W., van Wijngaarden, E., Dye, T.D., Cook, S., Swan, S.H., 2007. Concentrations of urinary phthalate metabolites are associated with increased waist circumference and insulin resistance in adult U.S. males. Environ. Health Perspect. 115, 876–882.

Stanner, S.A., Yudkin, J.S., 2001. Fetal programming and the Leningrad Siege study. Twin Res. 4, 287–292.

Suryawan, A., Hu, C.Y., 1993. Effect of serum on differentiation of porcine adipose stromal-vascular cells in primary culture. Comp. Biochem. Physiol. Comp. Physiol. 105, 485–492.

Swan, S.H., 2008. Environmental phthalate exposure in relation to reproductive outcomes and other health endpoints in humans. Environ. Res. 108, 177–184.

Swinburn, B.A., Sacks, G., Hall, K.D., McPherson, K., Finegood, D.T., Moodie, M.L., Gortmaker, S.L., 2011. The global obesity pandemic: shaped by global drivers and local environments. Lancet 378, 804–814.

Tamori, Y., Masugi, J., Nishino, N., Kasuga, M., 2002. Role of peroxisome proliferator-activated receptor-gamma in maintenance of the characteristics of mature 3T3-L1 adipocytes. Diabetes 51, 2045–2055.

Taxvig, C., Dreisig, K., Boberg, J., Nellemann, C., Schelde, A.B., Pedersen, D., Boergesen, M., Mandrup, S., Vinggaard, A.M., 2012. Differential effects of environmental chemicals and food contaminants on adipogenesis, biomarker release and PPARgamma activation. Mol. Cell. Endocrinol. 361, 106–115.

Teitelbaum, S.L., Mervish, N., Moshier, E.L., Vangeepuram, N., Galvez, M.P., Calafat, A.M., Silva, M.J., Brenner, B.L., Wolff, M.S., 2012. Associations between phthalate metabolite urinary concentrations and body size measures in New York City children. Environ. Res. 112, 186–193.

Trasande, L., Attina, T.M., Sathyanarayana, S., Spanier, A.J., Blustein, J., 2013. Race/ethnicity-specific associations of urinary phthalates with childhood body mass in a nationally representative sample. Environ. Health Perspect. 121, 501–506.

Wang, Y.F., Chao, H.R., Wu, C.H., Tseng, C.H., Kuo, Y.T., Tsou, T.C., 2010. A recombinant peroxisome proliferator response element-driven luciferase assay for evaluation of potential environmental obesogens. Biotechnol. Lett. 32, 1789–1796.

Weiss, B., 2012. The intersection of neurotoxicology and endocrine disruption. Neurotoxicology 33, 1410–1419.

Whyatt, R.M., Perzanowski, M.S., Just, A.C., Rundle, A.G., Donohue, K.M., Calafat, A.M., Hoepner, L.A., Perera, F.P., Miller, R.L., 2014. Asthma in inner-city children at 5–11 years of age and prenatal exposure to phthalates: the Columbia center for Children's environmental Health cohort. Environ. Health Perspect. 122, 1141–1146.

Wittassek, M., Angerer, J., 2008. Phthalates: metabolism and exposure. Int. J. Androl. 31, 131–138.

Wolff, M.S., Teitelbaum, S.L., McGovern, K., Windham, G.C., Pinney, S.M., Galvez, M., Calafat, A.M., Kushi, L.H., Biro, F.M., Breast, C., Environment Research, P., 2014. Phthalate exposure and pubertal development in a longitudinal study of US girls. Hum. Reprod. 29, 1558–1566.

Xie, B., Waters, M.J., Schirra, H.J., 2012. Investigating potential mechanisms of obesity by metabolomics. J. Biomed. Biotechnol. 2012, 805683.

Yaghjyan, L., Sites, S., Ruan, Y., Chang, S.H., 2015. Associations of urinary phthalates with body mass index, waist circumference and serum lipids among females: National Health and Nutrition Examination Survey 1999–2004. Int. J. Obes.

Yin, L., Dale, B.A., 2007. Activation of protective responses in oral epithelial cells by *Fusobacterium nucleatum* and human beta-defensin-2. J. Med. Microbiol. 56, 976–987.

Yu, X., Hong, S., Moreira, E.G., Faustman, E.M., 2009. Improving in vitro sertoli cell/gonocyte co-culture model for assessing male reproductive toxicity: lessons learned from comparisons of cytotoxicity versus genomic responses to phthalates. Toxicol. Appl. Pharmacol. 239, 325–336.

Zebisch, K., Voigt, V., Wabitsch, M., Brandsch, M., 2012. Protocol for effective differentiation of 3T3-L1 cells to adipocytes. Anal. Biochem. 425, 88–90.